

# Synthesis/Characterization and Novel Applications of Molecular Sieve Materials

Symposium held May 1-3, 1991, Anaheim, California, U.S.A.

EDITORS:

**Robert L. Bedard**

UOP, Tarrytown, New York, U.S.A.

**Thomas Bein**

Purdue University, West Lafayette, Indiana, U.S.A.

**Mark E. Davis**

California Institute of Technology, Pasadena, California, U.S.A.

**Juan Garces**

Dow Chemical Company, Midland, Michigan, U.S.A.

**Victor A. Maroni**

Argonne National Laboratory, Argonne, Illinois, U.S.A.

**Galen D. Stucky**

University of California at Santa Barbara, Santa Barbara, California, U.S.A.



MATERIALS RESEARCH SOCIETY  
Pittsburgh, Pennsylvania

1991

# Contents

PREFACE	ix
MATERIALS RESEARCH SOCIETY SYMPOSIUM PROCEEDINGS	x
PART I: MOLECULAR SIEVE CATALYSIS	
*CRACKING AND AROMATIZATION OF BUTANES OVER ZSM-5 ZEOLITES Yoshio Ono, Kunihiko Kanae, Kazuaki Osako, and Katsumi Nakashiro	3
*PREPARATION, CHARACTERIZATION AND ACTIVITY OF MOLECULAR SIEVE MATERIAL AS BASE CATALYSTS Avelino Corma	17
*NOVEL AND PROMISING APPLICATIONS OF MOLECULAR SIEVES IN ORGANIC SYNTHESIS AND THEIR CONTRIBUTION TO ENVIRONMENTAL PROTECTION Wolfgang F. Hoelderich	27
SELECTIVE OXIDATION OF HYDROCARBONS BY COBALT-SUBSTITUTED ALUMINOPHOSPHATE MOLECULAR SIEVES Victor A. Maroni and Lennox E. Iton	37
PART II: SYNTHESIS OF ZEOLITES, $AlPO_4s$ , AND LAYERED MOLECULAR SIEVES	
*DIRECTING EFFECT OF FLUORIDE IN THE SYNTHESIS OF MOLECULAR SIEVES WITH NEW CHARACTERISTICS AND OF THE FIRST TWENTY-MEMBERED RING MICROPOROUS SOLID Henri Kessler	47
COBALT AS A PROBE ION IN THE SYNTHESIS OF $CoAPO-5$ M.G. Uytterhoeven, W.A. Van Keyenberg, and R.A. Schoonheydt	57
*SYSTEMATIC PREPARATION OF POLYOXOMETALATE PILLARED LAYERED DOUBLE HYDROXIDES VIA DIRECT AQUEOUS REACTION Jiandang Wang, Ying Tian, Ren-Chain Wang, Jorge L. Colón, and Abraham Clearfield	63
SYNTHESIS AND CHARACTERIZATION OF PILLARED ACID- ACTIVATED MONTMORILLONITES Robert Mokaya, William Jones, Mavis E. Whittle, and Mary E. Davies	81
PREPARATION OF MONTMORILLONITE- <i>p</i> -AMINOAZOBENZENE INTERCALATION COMPOUNDS AND THEIR PHOTOCHEMICAL BEHAVIOR Makoto Ogawa, Keiko Fujii, Kazuyuki Kuroda, and Chuzo Kato	89
*Invited Paper	

ZIRCONIUM ORGANIC DIPHOSPHATE-DIPHOSPHONATES WITH  
TILTED RIGID PILLARS 95  
G. Alberti, U. Costantino, R. Vivani, and  
P. Zappelli

PREPARATION OF ZIRCONIUM DIPHOSPHONATE-PHOSPHITES WITH  
A NARROW DISTRIBUTION OF MESOPORES 101  
G. Alberti, U. Costantino, R. Vivani, and  
P. Zappelli

PART III: NOVEL OPTICAL, ELECTRICAL,  
AND SENSOR MATERIALS

\*DOPING AND BAND-GAP ENGINEERING OF AN INTRAZEOLITE  
TUNGSTEN(VI) OXIDE SUPRALATTICE 109  
Geoffrey A. Ozin, Andrzej Malek, Richard  
Prokopowicz, Peter M. Macdonald, Saim Özkar,  
Karin Moller, and Thomas Bein

\*PHOTOCHEMISTRY AND PHOTOPHYSICS OF MATERIALS IN ZEOLITES 119  
Kai-Kong Iu, Xincheng Liu, and J. Kerry Thomas

GROWTH, SIZE AND PHOTOACTIVITY OF CdS, ZnS, OR PbS  
PARTICLES IN NaX ZEOLITE 133  
M. Wark, G. Schulz-Ekloff, N.I. Jaeger, and  
W. Lutz

PbI<sub>2</sub> CONFINED IN THE SPACES OF LTA ZEOLITES 139  
O. Terasaki, Z.K. Tang, Y. Nozue, and T. Goto

\*ZEOLITIC MATERIALS AS ORGANIZING MEDIA FOR SEMI-  
CONDUCTOR-BASED ARTIFICIAL PHOTOSYNTHETIC SYSTEMS 145  
Yeong Il Kim, Richard L. Riley, Munir J. Huq,  
Samer Salim, Angie N. Le, and Thomas E. Mallouk

\*MOLECULAR DESIGN OF ALUMINOSILICATE THIN FILM DEVICES 157  
Kenneth E. Creasy, Ying Ping Deng, Jongman Park,  
Eric V.R. Borgstedt, Shawn P. Davis, Steven L.  
Suib, and Brenda R. Shaw

PHOTOREDUCTION OF METHYLVIOLOGEN IN THE INTERLAYERS OF  
SOME LAYERED TITANATES AND NIOBATES 169  
Teruyuki Nakato, Yoshiyuki Sugahara, Kazuyuki  
Kuroda, and Chuzo Kato

ZEOLITE CRYSTAL LAYERS COUPLED TO PIEZOELECTRIC  
SENSORS: MOLECULAR RECOGNITION DEVICES 175  
Yongan Yan and Thomas Bein

PART IV: SYNTHESIS DIRECTED  
TO SPECIAL APPLICATIONS

\*INTERCALATION OF LAYERED V<sub>2</sub>O<sub>5</sub> XEROGEL WITH POLYMERS 183  
M.G. Kanatzidis, C.-G. Wu, Y.-J. Liu,  
D.C. DeGroot, J.L. Schindler, H.O. Marcy,  
and C.R. Kannewurf

\*Invited Paper

SURFACE CHEMISTRY OF HETEROBIMETALLIC Ge-M (M = Mo,W) COMPLEXES IN ZEOLITE Y	195
Aticha Borvornwattananont, Karin Moller, and Thomas Bein	
FORMATION AND CHARACTERIZATION OF SULFIDE CLUSTERS IN MOLECULAR SIEVE ZEOLITE MATERIALS	201
Markus Winterer, Lennox E. Iton, Stanley A. Johnson, and Victor A. Maroni	
REDUCTION OF Cu <sup>2+</sup> AND Ni <sup>2+</sup> IN ZEOLITE Y USING POLYOL PROCESS: A NEW APPROACH IN THE PREPARATION OF METAL SUPPORTED CATALYSTS	207
P.B. Malla, P. Ravindranathan, S. Komarneni, E. Breval, and R. Roy	
DESIGNING ZEOLITES AS NOVEL PRECURSORS TO ELECTRONIC CERAMICS	213
David R. Corbin, John B. Parise, Uma Chowdhry, and M.A. Subramanian	
NANOSCALE ENGINEERED CERAMICS FROM ZEOLITES: CREATING THE IDEAL PRECURSOR FOR HIGH-QUALITY CORDIERITE	219
Robert L. Bedard and Edith M. Flanigen	
THE APPLICATION OF MOLECULAR SIEVES AS MAGNETIC RESONANCE IMAGING CONTRAST AGENTS	225
Kenneth J. Balkus, Jr., Iwona Bresinska, Stanislaw Kowalak, and Stuart W. Young	
PREPARATION OF CERAMIC MOLECULAR SIEVE MEMBRANES	231
E.R. Geus, J. Schoonman, and H. van Bekkum	
SYNTHESIS AND WATER SORPTION PROPERTIES OF ALUMINO- PHOSPHATE (AlPO <sub>4</sub> ) AND SILICOALUMINOPHOSPHATE (SAPO) MOLECULAR SIEVES	237
P.B. Malla and S. Komarneni	
PART V: NOVEL SYNTHETIC AND CHARACTERIZATION METHODS	
*THE PHYSICOCHEMICAL PROPERTIES OF VPI-7: A MICROPOROUS ZINCOSILICATE WITH THREE-MEMBERED RINGS	245
Michael J. Annen, Mark E. Davis, John B. Higgins, and John L. Schlenker	
*THE HYDROTHERMAL SYNTHESIS OF LAYERED MOLYBDENUM PHOSPHATES WITH OCTAHEDRAL-TETRAHEDRAL LAYERS	255
Robert C. Haushalter and Linda A. Mundi	
FLEXIBILITY OF THE ZEOLITE RHO FRAMEWORK: THE REDISTRIBUTION OF EXTRA FRAMEWORK CATIONS AS A FUNCTION OF TEMPERATURE	267
John B. Parise, Xing Liu, David R. Corbin, and Glover A. Jones	

\*Invited Paper

LOW TEMPERATURE STUDIES OF RARE GASES ADSORBED ON MOLECULAR SIEVE MATERIALS	273
Graham F. McCann, I. Gameson, W.J. Stead, T. Rayment, P.J. Barrie, and J. Klinowski	
<sup>129</sup> XE NMR AS A PROBE OF MICROPOROUS MATERIALS	281
John A. Ripmeester and Christopher I. Ratcliffe	
ATOMIC FORCE MICROSCOPY OF MICRON SIZE SILICALITE CRYSTALS	287
P. Rasch, W.M. Heckl, H.W. Deckman, and W. Häberle	
STRUCTURAL CHARACTERIZATION OF ZEOLITES USING RAMAN SCATTERING	295
H.W. Deckman, J.A. Creighton, R.G. Buckley, and J.M. Newsam	
AUTHOR INDEX	301
SUBJECT INDEX	303

**ZEOLITE CRYSTAL LAYERS COUPLED TO PIEZOELECTRIC SENSORS:  
MOLECULAR RECOGNITION DEVICES**

YONGAN YAN AND THOMAS BEIN\*

Department of Chemistry, University of New Mexico, Albuquerque, NM 87131, USA

**ABSTRACT**

Microporous zeolite crystals were successfully coupled onto the gold electrodes of quartz crystal microbalances (QCM). A self-assembled monolayer of thiol-alkoxysilane coupling agent on the gold surface was used as the interfacial layer to promote adhesion of the zeolite crystals to the QCM. The resulting, densely packed single layers of zeolite crystals were stable to at least 625 K. Transient sorption behavior of organic vapor pulses, dynamic vapor sorption isotherms and nitrogen sorption isotherms at liquid nitrogen temperature were examined to characterize the zeolite-coated QCMs. Depending on the type of zeolite coating, the resonance frequency response to vapor pulses could be increased up to 500-fold compared to the bare QCM. The regular micropores (0.3-0.8 nm) of the QCM-attached zeolite crystals were found to control molecular access into the extensive intrazeolite volume. Selectivity of the frequency response in excess of 100:1 toward molecules of different size and/or shape could be demonstrated. An additional recognition mechanism based upon intrazeolite diffusion rates was also established.

**INTRODUCTION**

Much effort has been devoted to design coatings for microsensors<sup>1,2,3</sup> such as optical waveguides, chemically sensitive field effect transistors, chemiresistors and acoustic wave devices. Our recent development of molecular sieve-based composite films has introduced a novel means for controlling vapor/surface interactions.<sup>1,4,5,6</sup> A sensor coated with molecular sieve crystals discriminates different molecules according to their sizes and shapes, with the ability to fine-tune pore opening sizes in the range of 0.3-1.2 nm. Our previous work was focused on zeolite/glass microcomposites derived from sol/gel suspensions and coated on surface acoustic wave devices.

In this study we demonstrate the selective adsorption behavior of well-defined single layer zeolite crystal coatings on the gold electrodes of quartz crystal microbalances (QCM). The coupling agent 3-mercaptopropyltrimethoxysilane, HS(CH<sub>2</sub>)<sub>3</sub>Si(OCH<sub>3</sub>)<sub>3</sub>, was used as a bifunctional molecular precursor for anchoring zeolite crystals to the gold electrode. Gold shows strong specific interactions with thiol groups that permit formation of self-assembled monolayers in the presence of many other functional groups.<sup>7,8</sup> Figure 1 summarizes the idealized process of the formation of a zeolite-coated QCM. We note that a small degree of hydrolysis of the methoxy groups and condensation of the thiols could lead to the deposition of some oligomers on the surface. Due to the vastly different dimensions of the zeolite crystals and the interface layer, this will not have a noticeable effect on the structure of the film. A related system consisting of SnO<sub>2</sub>/cationic disilane/zeolite arrangements has been reported for the self-assembly of redox chains at electrodes.<sup>9</sup>

The QCM consists of a piezoelectric quartz substrate with electrodes deposited on opposite surfaces of the crystal. Mass changes  $\Delta m$  (in g) on the surface of the QCM cause proportional shifts  $\Delta f$  of the fundamental resonance frequency  $F$ , according to

$$\Delta f = -2.3 \times 10^{-6} F^2 \Delta m / A$$

where  $A$  is the electrode surface area (in cm<sup>2</sup>). Therefore the 9 or 5 MHz QCM is capable of detection of mass changes at the nanogram level.<sup>10,11</sup> Two types of surface area are present on the zeolite-coated QCM electrodes: the external surface area which consists of the zeolitic external surface and the interfacial surface exposed to the gas phase, and the internal zeolite surface area. Access to the zeolite interior is controlled by the pore opening size of the crystalline material. If 90% of the electrode is covered by 5  $\mu$ m crystals of CaA zeolite, the ratio of N<sub>2</sub> sorption at liquid nitrogen temperature on the internal and external surface would be expected to be over 1000.<sup>12</sup> This value provides an

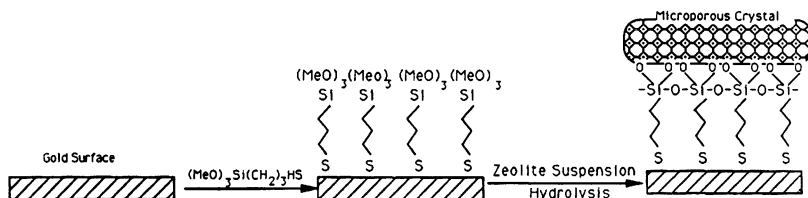


**Figure 1.** Anchoring of zeolite crystals on gold surface via the thiol-alkoxysilane coupling interfacial layer.

estimate for the possible discrimination/selectivity of organic vapors to be expected on the coated QCM.

## EXPERIMENTAL SECTION

**Materials.** Sodium zeolite Y with  $\text{SiO}_2/\text{Al}_2\text{O}_3$  molar ratio of 4.74, and silicalite with  $\text{SiO}_2$  content > 99% were obtained from Union Carbide and used as received. Potassium A zeolite was obtained by exchange of 4A zeolite (Alfa) with 1N aqueous solution of KCl and subsequent filtering and washing with water.  $\text{HS}(\text{CH}_2)_3\text{Si}(\text{OCH}_3)_3$  (Aldrich) was used without further purification. Toluene and hexadecane (Fisher) were stored over dehydrated 3A zeolite, and deoxygenated by bubbling  $\text{N}_2$  for 30 minutes when employed as solvents for the formation of organosilane-thiol monolayers.

**Anchoring of zeolite crystals to gold surfaces.** The vacuum-deposited gold electrodes on the AT-cut 5 MHz QCM's acquired from ICM-Crystal Division (Oklahoma) were used for zeolite coating, porosity characterization, and selectivity studies with different organic vapors. The gold substrates were plasma-cleaned before use. The anchoring of zeolite crystals to the gold surface involved two steps: formation of an interfacial monolayer and exposure to a zeolite suspension in toluene or acetonitrile. The interfacial monolayer was spontaneously formed by immersing the gold substrate into 1.0-5.0 mM 3-mercaptopropyltrimethoxysilane solution in dry hexadecane or toluene.<sup>13</sup> The monolayer-covered substrates were stirred overnight with zeolite suspensions in toluene or acetonitrile.

## Characterization of coating porosity

### (a) Sorption of vapor pulses.

The response of the zeolite-coated QCM's to different organic vapors was examined with the apparatus schematically shown in Figure 2. This instrument consists of a gas inlet and signal output system. A carrier gas (He or  $\text{N}_2$ ), purified by passing through a molecular sieve trap, continuously purges the injection port and detector cell. All zeolite-coated QCM's were heated to 473 K to remove water prior to use. IR spectroscopic and sorption measurements established that this treatment reduces the water content below

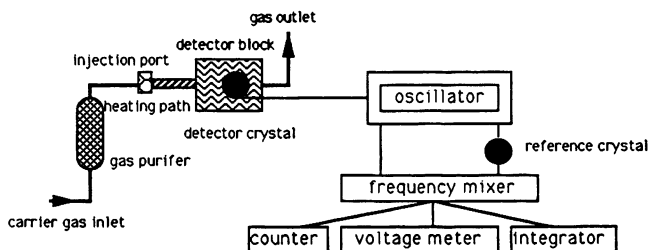


**Figure 2.** Schematic diagram of the apparatus for transient sorption of vapor pulses by zeolite coated QCM

detection level. The organic sample (0.5  $\mu\text{l}$ ) is injected through a temperature-controlled injection port, whose temperature is 30-50 K higher than the detector block to ensure fast evaporation and avoid condensation. The vapor leaving from the injection port is then detected by a coated QCM crystal in a 1 ml sealed cell. The frequency variation was monitored by heterodyning the detector signal against a reference oscillating circuit through a frequency mixer, and converting the frequency to an analog voltage. The frequency output was simultaneously monitored by a frequency counter (HP 5384A) and recorded by an integrator (HP 3380A). The QCM-response to vapor pulses was compared with that of a thermal conductivity detector (TCD) in series with the QCM (Sigma gas chromatograph).

(b) Dynamic sorption isotherms

Vapor sorption isotherms were measured at 373 K with the above arrangement that was modified for vapor flow. The injection port was replaced by a direct inlet for a nitrogen flow with different vapor concentrations prepared in a diffusion cell with mass flow controllers. Nitrogen adsorption isotherms were obtained at 77K in a second gas dosing system with computer-adjusted mass flow controllers (UNIT). The nitrogen partial pressure in helium was adjusted over the range of 0-0.899.

## RESULTS AND DISCUSSION

SEM micrographs of the zeolite-coated gold surfaces show that this coating process provides uniform crystal distributions on the entire substrate surface. The coating phases also display the crystalline habit of the bulk materials. We note that the coating process is independent of the slide orientation in the suspension, *i.e.*, whether the slide is oriented vertically or at an acute angle. It was also observed that no zeolite crystals attached on the fresh gold surface without the silane-thiol interfacial layer. For the thermally treated slides, a fraction of the zeolite coating can survive low power ultrasonication. When the zeolite-coated QCM was heated to 530 K, no detectable mass change was observed after re-equilibration in air.

### Sorption and desorption response of zeolite-coated quartz microbalances

#### A. Transient vapor sorption

The transient adsorption of a group of different organic vapor pulses on zeolite 3A, Y and silicalite-coated quartz microbalances was studied. The pore opening sizes of these microporous coatings vary from the partially potassium blocked, 8 oxygen-membered ring of 3A zeolite (0.3 nm), to 10 membered silicalite (0.55 nm), and sodium Y zeolite with 12-membered rings (0.75 nm). The Si/Al ratios differ from 1.0 for A zeolite, 2.4 for Y zeolite, to ca. 100 for silicalite. The intrazeolite surface changes from hydrophilic to more hydrophobic in the same sequence.<sup>14</sup> Figure 3 shows the frequency response shifts of the silicalite-coated QCM upon sequential injection of 0.5  $\mu\text{l}$  of different organics. For comparison, the signal responses of the thermal conductivity detector (TCD) and of the bare QCM to the same injections are also illustrated. The TCD traces show that the tails observed in the QCM response to many vapors are not due to the mixing time constant of the QCM cell.

It is obvious that the QCM frequency responses to the probe molecules differ drastically. The frequency shifts typically increase when the probe molecular diameters decrease. If the response of the silicalite layer to water (0.265nm) and isooctane (0.62nm) is compared, the discrimination ratio of the molecules admitted and rejected from the coatings is in excess of 100:1. It is observed that in the case of molecules with kinetic diameters smaller than the zeolite pore size, the organic vapors are desorbed more slowly from the QCM cell as indicated by the TCD response (The TCD was mounted in series with the QCM). It is therefore suggested that the desorption tails result from the activated diffusion/desorption process of the probe molecules from the constricted microporous system. Molecules with sizes close to those of the zeolite pores desorb more slowly than smaller ones. The response magnitude and the sorption-desorption kinetics are a function of the amount of vapor in the pulse, the velocity and temperature of purge gas, and treatment of the coated QCM. At identical conditions, the peak shapes exhibited by the microporous system reflect physical properties of the probe molecules, such as molecular



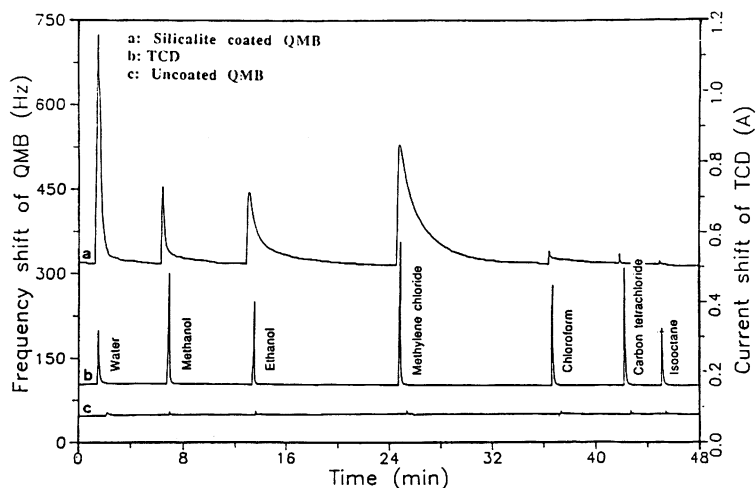


**Figure 3.** Transient sorption of vapor pulses on silicalite-coated QMB at 373 K.

shape, size and polarizability. Therefore, this response pattern offers an additional means of molecular identification.

With increasing zeolite pore size, the sodium Y zeolite coated QCM shows a significant increase in the frequency response. The frequency response is nearly 500 times that of an uncoated QCM. For the molecules examined in this study, zeolite Y does not exhibit strong selectivity. This is due to the large pore diameter of Y crystals (0.75 nm).

### B. Adsorption isotherms

In order to provide further insight into the nature of sorption of the probe molecules in the zeolite layers, adsorption isotherms at very low partial pressures  $p/p_0$  were measured in a stream of diluted organic vapors at 323 K, and with nitrogen at 77 K. Figure 4 shows the dynamic sorption isotherms of water and isooctane on zeolite 3A, Y and silicalite-coated quartz microbalances.

Due to its small molecular size and high polarity, the adsorption of water in the microporous materials at low partial pressure is substantial (Figure 4a). The adsorption capacity of the coating layers shows a sequence Y zeolite > 3A zeolite > silicalite. This sequence is consistent with the available microporous volume of the coating material.<sup>15</sup> In this dynamic sorption system the noise of the frequency variation was usually limited to 0.5 Hz, while the frequency response to the vapor sorption was as large as 700 Hz. In contrast to the behavior of bulk zeolite materials, the adsorption of water on the single-layer polar zeolite films such as Y and 3A zeolite is characterized by reversible adsorption-desorption isotherms with fast equilibration at 373 K. Complete desorption of water can be achieved at 393 K in less than 5 min, and the sorption equilibrium of the isotherm can be reached in 30s irrespective of the types of zeolite.

The adsorption isotherms of n-decane (not shown) demonstrate both the molecular sieve effect and the influence of the interaction energy on the sorption capacity in the microporous materials. In the range of experimental conditions the sorption capacity shows the sequence silicalite > Y zeolite >> 3A zeolite. If the isotherm shapes are compared, it is found that at lower partial pressure, the sorption capacity of silicalite is larger than that of Y-zeolite. This can be attributed to the organophilic character of the silicalite. As a result of molecular exclusion from the internal pore volume, a very low sorption capacity of n-decane on 3A zeolite is observed. The ratio of n-decane sorption on silicate and 3A zeolite as a function of vapor concentration becomes larger at lower concentration. This observation is in agreement with the multiple micropore filling mechanism,<sup>16,17</sup> *i.e.* the highest adsorption potential is involved in the smallest micropores compared with larger pores and the external surface. Thus the adsorption of vapor at lower pressure would

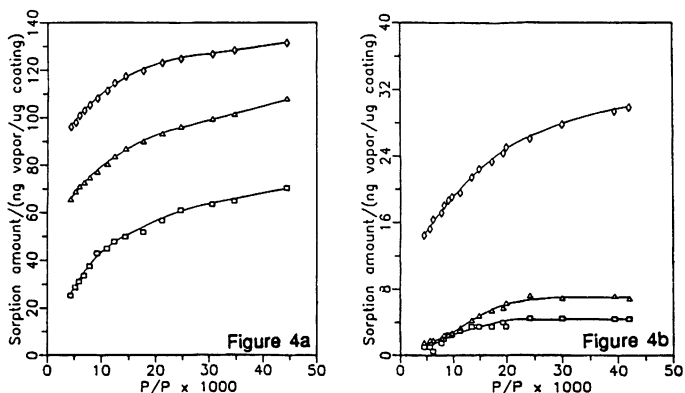


**Figure 4.** Dynamic sorption isotherms of water (Figure 4a), and isooctane (Figure 4b) on QMBs coated with silicalite ( $\square$ ); Y zeolite ( $\diamond$ ) and 3A zeolite ( $\Delta$ ) at 373 K.

preferentially take place in the microporous system over the external surface of the zeolite. These results suggest that higher molecular size-based selectivity and larger sorption capacity (sensitivity) compared to amorphous surfaces can be achieved at the lowest vapor concentration.

On increasing the probe molecular size, effective exclusion of isooctane was observed on QMBs both coated with silicalite and 3A zeolite (Figure 4b). The sorption capacity of isooctane in the zeolite Y film is smaller than that for water. Such behavior results partially from the sodalite cages in the Y structure that are not accessible to isooctane, and partially from less effective packing of the large isooctane in zeolite Y (the adsorbed amount of isooctane in bulk NaY is about 50% that of water at 298 K<sup>14</sup>).

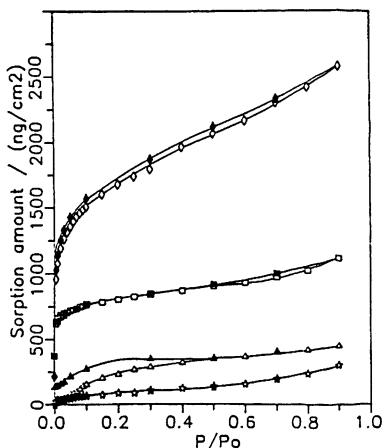


**Figure 5.** Sorption isotherms of nitrogen at 77K on QMBs coated with silicalite ( $\square$ ); Y zeolite ( $\diamond$ ); 3A zeolite ( $\Delta$ ) and bare QMB ( $\star$ ). Open and filled symbols designate sorption and desorption points, respectively.

Figure 5 shows the corresponding adsorption isotherms of nitrogen at 77 K. The sorption on QMBs coated with Y zeolite and silicalite exhibits a reversible isotherm with very little hysteresis, which suggests that no mesopores are present in the coating. However, it requires a long time (over several hours) to return back to zero nitrogen

loading at zero nitrogen pressure during the completion of the desorption process. On QCM's coated with 3A zeolite, a hysteresis was observed over the lower pressure range, which possibly indicates that some material with pores larger than the parent-3A zeolite is present in the coating, as complete exclusion of nitrogen at 77K should be expected in this zeolite. If the sorption capacity of a 3A-coated and a bare QCM is compared, we find that the zeolite coating does not remarkably increase the external surface area of the QCM's electrode. Thus the non-selective adsorption in the coatings should be very small.

## CONCLUSION

The zeolite-coated QCM can be used to monitor microporous adsorption behavior at very low vapor concentrations in a dynamic flow system. The high vapor sorption capacity of the microporous coatings and the molecular size and shape-based selectivity at very low concentrations show that such a combination has great potential for designing highly sensitive and selective chemical sensors.

## ACKNOWLEDGEMENT

The authors thank the National Science Foundation and the Department of Energy for funding of this research. We appreciate the assistance of Kelly Brown and Ray Forrister (UNM) during various phases of this study.

## REFERENCES

- 1 Bein, T.; Brown, K.; Frye, G. C.; Brinker, C. J., *J. Am. Chem. Soc.*, 1989, 111, 7640.
- 2 "Solid State Chemical Sensors", Janata, J.; Huter, R. J., Eds.; Academic: Orlando, FL, 1985.
- 3 "Fundamentals and Applications of Chemical Sensors", Schuetzle, D.; Hammerle, R., Eds., ACS Symposium Series 309: Washington, D.C., 1988.
- 4 Bein, T.; Brown, K.; Enzel, P.; Brinker, C. J., *Mat. Res. Soc. Symp. Proc.*; Materials Research Soc. Pittsburgh, 1988, 121, 761.
- 5 Bein, T.; Brown, K.; Brinker, C. J., *Stud. Surf. Sci. Catal.* 49, Jacobs, P. A. and van Santen, R. A.; Eds.; Elsevier, Amsterdam, 1989, p.887.
- 6 Bein, T.; Brown, K.; Brinker, C. J., *J. Non-Cryst. Solids*, in press.
- 7 Bain, C. D.; Troughton, E. B.; Tao, Y. T.; Evall, J.; Whitesides, G. M.; Nuzzo, R. G., *J. Am. Chem. Soc.*, 1989, 111, 321.
- 8 Porter, M. D.; Bright, T. B.; Allara, D. L.; Chidsey, C. E. D., *J. Am. Chem. Soc.*, 1987, 109, 3559.
- 9 Li, Z.; Lai, C.; Mallouk, T. E. *Inorg. Chem.*, 1989, 28, 178.
- 10 The 5 MHz QCM used in this experiment has a total electrode area of 0.72 cm<sup>2</sup>; a frequency shift of 1 Hz corresponds to a mass change of 12.5 ng on the QCM.
- 11 Ballantine, D. S.; Wohltjen, H., *Anal. Chem.*, 1989, 612(11), 704A.
- 12 This calculation is based on nitrogen adsorption capacity of 0.239 g/g for CaA, and a dense monolayer packing of nitrogen (1.62nm<sup>2</sup>) on the external surface at liquid nitrogen temperature.
- 13 Troughton, E. B.; Bain, C. B.; Whitesides, G. M.; Nuzzo, R. G.; Allara, D. L. and Porter, M. D., *Langmuir*, 1988, 4, 365.
- 14 Barrer, R. M., "Hydrothermal Chemistry of Zeolites", Academic; NY, 1982.
- 15 Breck, D. W., "Zeolite Molecular Sieves", Krieger, Malabar, FL, 1984.
- 16 Carrott, P. J. M.; Roberts, R. A. and Sing, K. S. W. in "Characterization of Porous Solids", Ed. Unger, K. K.; Rouquerol, J.; Sing, K. S. W. and Kral, H., Elsevier, Amsterdam, 1988, p. 88.
- 17 Kakei, K.; Ozeki, S.; Suzuki, T. and Kaneko, K., *J. Chem. Soc., Faraday Trans. 1*, 1990, 80(2), 371.